Compression of Snow at Constant Speed*

Seiiti KINOSITA
木 下 誠 一
The Institute of Low Temperature Science
Hokkaido University, Sapporo, Japan

Abstract

Snow is a kind of visco-elastic material. Its mode of deformation is strongly influenced by the deformation speed: Slow speed produces plastic deformation, while high speed produces brittle fracture. The difference is due to the change of internal texture of snow during the deformation: The plasticity is accompanied by the dislocation within the ice grains forming the network connections with each other, while the brittleness is accompanied by the disjointment of the connections.

In the case of compression the critical transition speed from plasticity to brittleness is several mm/min and changes slightly with the temperature and the density of snow.

Experiments were carried out by compressing uniaxially a snow cylinder or forcing a rigid cone into a snow block. The compression speeds used ranged very widely from 0.01 to 1 000 mm/min ($2\times10^{-5}\sim1.5$ cm/sec). In each experiment the external change along the whole snow mass and the microscopic internal change during the compression were observed. Compressive strengths or visco-elastic quantities were computed from the curves of the resistive force and related to the temperature, the density of snow and the compression speed.

By an extremely large plastic compression a snow cylinder was transformed into a thin ice plate. This experiment is comparable to the densification of snow in glacier or ice cap.

I. Introduction

Sometimes snow shows plasticity, and sometimes shows brittleness.

Snow deposited on the ground subsides gradually under the load of successively falling snow. At the depths of glacier or ice cap snow is progressively transformed into ice after the passing of innumerable years in the presence of a vast compression. This is one example of plastic deformation of snow at a slow speed compression.

In snow avalanches fractures propagate from one to another, as in a chain reaction, on the snow deposited along a slope. This is one example of brittle deformation of snow at a high speed compression.

It is a typical character for a visco-elastic material that the above-mentioned two different deformation modes (plasticity and brittleness) are developed at slow or high speed. Snow exerts such a mechanical behavior to its internal structure, namely network connections of ice grains, as shown in the photograph of Fig. 3 a. On plastic deformation internal changes take place mainly in dislocations within the ice grains, and on brittle deformation in disjointment of the network connections. The critical transition speed from plasticity to brittleness is several mm/min. This numerical value is important for snow.

* Contribution No. 784 from the Institute of Low Temperature Science.

In this paper the author has tried to formulate in a comprehensive way such a mechanical behavior of snow at constant speed compression.

II. Experimentation

Most of the experimental techniques and procedures have been given in detail elsewhere. Only a brief review will be given here.

Compressions of cylindrical snow samples were carried out by using a kind of unconfined compression apparatus (Kinosita, 1957, 1958). The speed was controlled by changing the reduction ratios between the gears and ranged very widely, from 0.001 to 1 000 mm/min. For an extremely large plastic compression an air-hydraulic type apparatus of 10 tons capacity was used because of the large resistive force (Kinosita, 1962).

In the experiment of forcing a rigid cone into a snow block, the snow block was set on the base of the unconfined compression apparatus, and the falling rod to which a rigid cone was attached to its end was forced into the snow (Kinosita, 1965).

The resistive force during the compression was recorded electrically by using a load cell of strain-gauge type.

In order to observe the external change along the whole snow mass during the compression, several ink stripes or lattices were marked previously along the side or the top surface of the cylindrical snow sample and the manner in which these figures changed with the progress of compression was observed from the side or the upper part (Figs. 2 a, b, c and d). After a rigid cone was forced into a snow block, the snow was cut vertically through the centre of the hole made in it, and the cut surface was sprayed with ink water, then exposed to heat; a 'spray figure' resulted disclosing the structure change produced in it (Figs. 2 e, f and g).

In order to investigate the internal change, thin sections were cut of both the original and the compressed snow, and observed under microscope (Figs. 3 a, b and c, 7 a, b and c) (Kinosita and Wakahama, 1960).

The experiments were conducted for compact snow deposited in Hokkaido. The density and the temperature of snow samples used ranged respectively from 0.15 to 0.45 g/cm^3 and from 0 to -30°C.

III. Schematic Illustration

Arranging the experimental results obtained to date, schematic representations are given in Fig. 1. In this figure external and internal changes of compressed snow, stress-strain and stress-speed relations during compression are shown for both plastic and brittle deformations.

Figure 1 (a) shows the external changes of a cylindrical snow sample (Kinosita, 1957). The left cylinder is an original one with several fine marks spaced at equal intervals on its side surface. The right cylinders are the compressed ones; the above is the plastically deformed (slow speed compression), while the below is the brittlely deformed (high speed compression). As may be seen from the changes of the side marks, the snow cylinder contracts uniformly along its whole length in plastic deformation (the photographs of Figs. 2 a and b), while it contracts not uniformly but in such a way that

it is broken down at its end portion and the remaining portion is unchanged in brittle deformation (the photographs of Figs. 2 c and d). Fractures take place intermittently at the top or the bottom of the snow cylinder, and ice grains taken to pieces are ejected and are piled up on the base or are packed in the centre of the end surface as shown by dotted regions.

Figure 1 (b) shows the microscopic internal changes of the network of ice grains A, B, C, D, E and F composing the snow. The left figure is the original network, and the right figures are the network after the compression; the above is after plastic deformation, and the lower is after brittle deformation. In the above figure basal slips occur within the ice grains A and D, and the grain boundary between B and C becomes curved (Kinosita, 1962). One example of such a basal slip within an ice grain composing the plastically compressed snow is shown in the photograph of Fig. 3 b. In Wakahama's experiments (Wakahama, 1960, 1966) it was shown that the main internal change in the plastically deformed snow is a basal slip within the ice grains composing it.

In the lower figure of Fig. 1 (b) disjointments of the connections between the ice

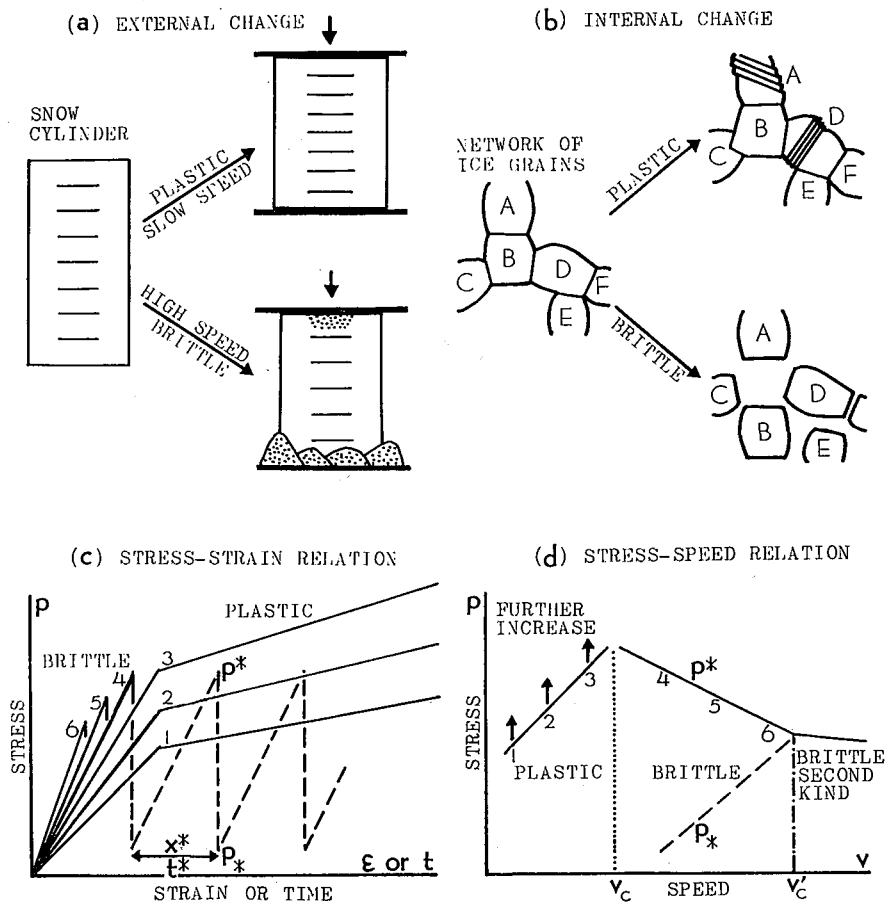

Fig. 1. Schematic illustration of the mechanical behavior of snow at constant speed compression

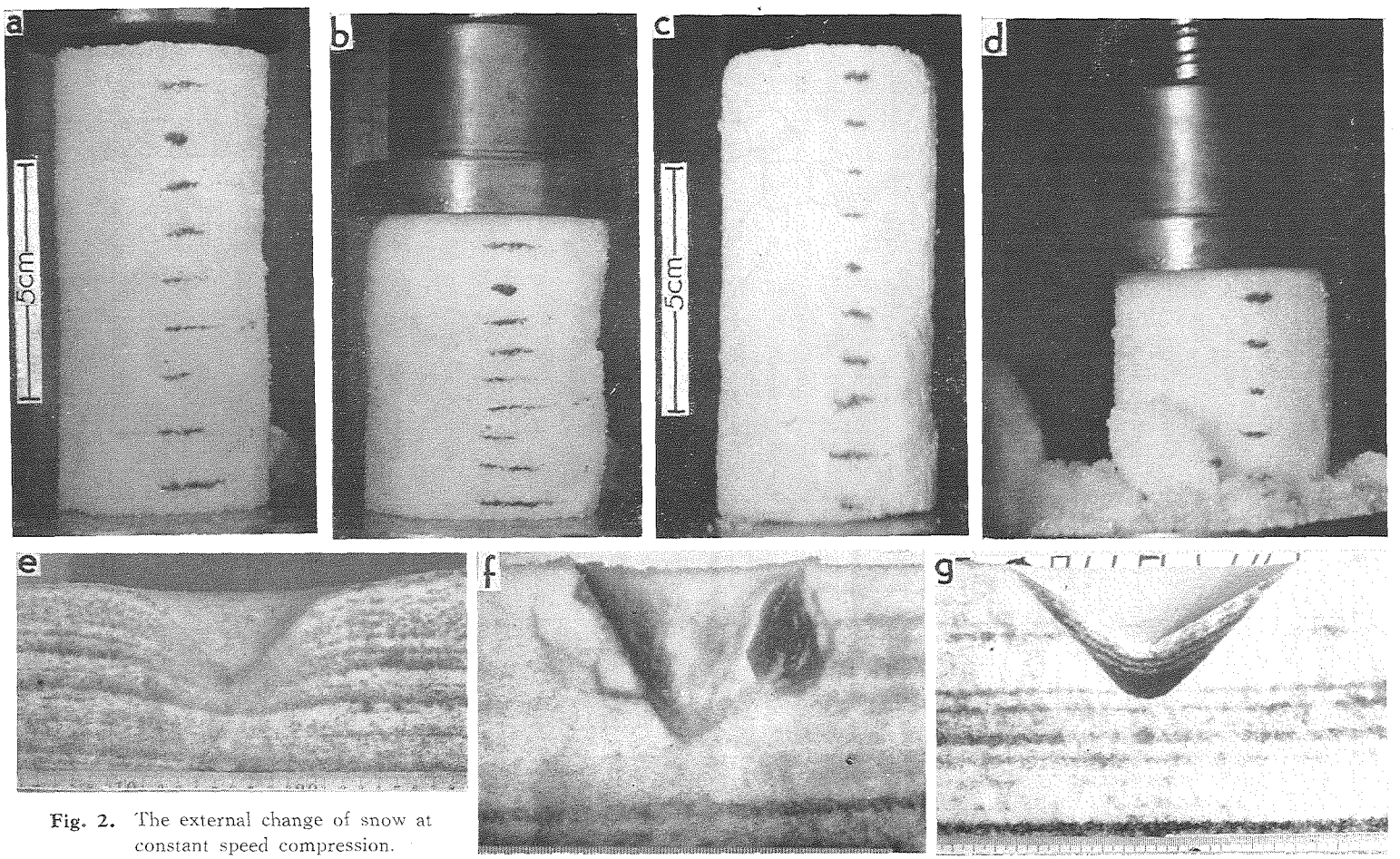

Fig. 2. The external change of snow at constant speed compression.
a, b: Plastic deformation of snow cylinder, a: Original, b: Final, c, d: Brittle deformation of snow cylinder, c: Original, d: Final, e, f, g: Spray figures on the cut surface of the snow block invaded by a rigid cone, e: Plastic deformation, apex angle $\theta = 90°$, f: Brittle deformation, $\theta = 60°$, g: Brittle deformation $\theta = 120°$

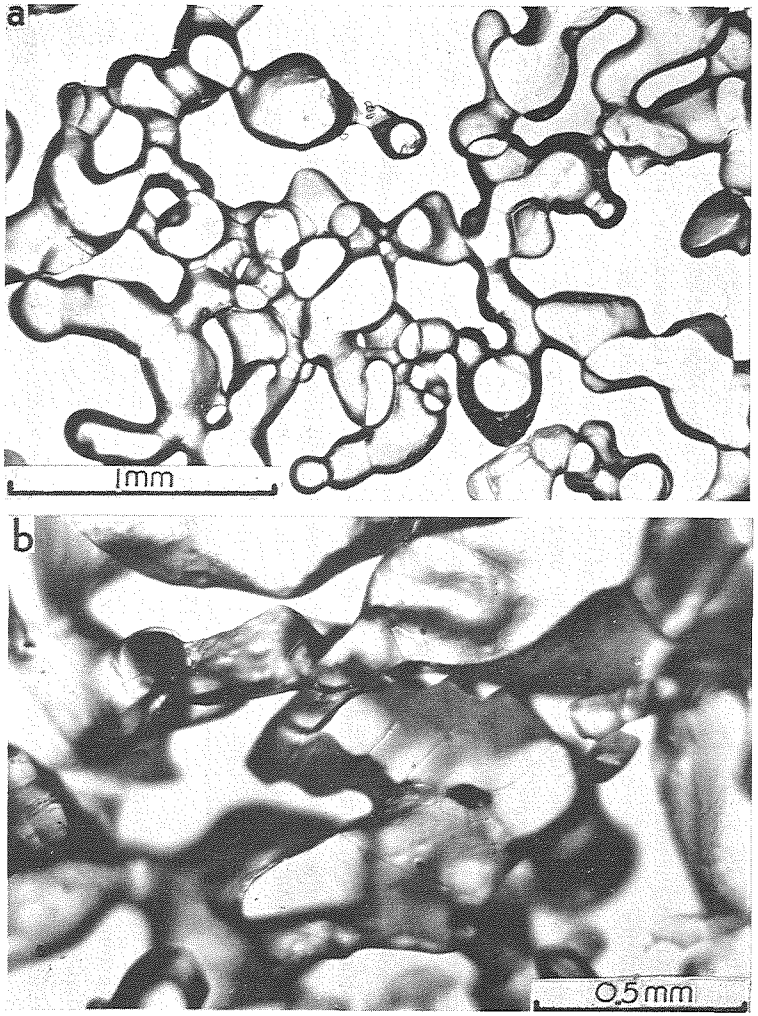

Fig. 3. Thin sections of snow.
a: Natural snow, density $\rho = 0.36\ g/cm^3$,
b: Basal slip appeared in an ice grain after plastic deformation, ρ, initial 0.38, final 0.56,
c: Ice grains broken to pieces after brittle deformation, $\rho = 0.27$

grains occur around all grain boundaries, and all ice grains are taken to piecess; the fracture takes place along the joints of the network (Kinosita, 1960, 1964). One example of such disjointment is shown in the photograph of Fig. 3 c.

The general feature of stress-strain relation is presented schematically by the diagram of Fig. 1 (c) (Kinosita, 1960), where the strain ε is defined as the ratio of the change in length to the original length. The numerals 1 to 6 attached to the lines stand in the increasing order to strain rate $\dot{\varepsilon}$ or compression speed v. The curves 1, 2 and 3 are given by plastic deformations. Stress p increases with strain ε, abruptly at a small strain (elastic region) and gently at a large strain (plastic region). The stress for the same strain becomes larger as the speed increases.

When the speed v exceeds a certain limit value v_c (the critical value is not the strain rate, but is rather the compression speed), brittle fracture occurs within a small strain and the stress p drops instantly from a maximum value p^* to a small value p_*. The curves 4, 5 and 6 are given by such brittle deformations. They may be roughly idealized by the straight lines, ending abruptly in fracture with no significant amount of plastic deformation. If the compression progresses further, stress increases again, and is almost nearly parallel to the previous increase, and at the same stress p^* fracture occurs again. In consequence stress-strain relation is given as a serrated shape of $p^* - p_*$ in breadth. The time t^* taken from one fracture to the next fracture becomes smaller as the speed v increases. The changes in length x^* during that time interval t^* (where $v = x^*/t^*$) is almost the same as the length of an ice grain. The inclination of the stress-strain curve becomes larger with the increasing speed, while the stress p^* at the fracture point becomes smaller.

Figure 1 (d) gives a schematic diagram of stress-speed relation. The numerals attached to the curve correspond to those for the stress-strain curves. In the region of plasticity, where $v < v_c$, the curve is drawn by connecting the values of yield stress. The yield occurs within 1% strain. The arrow marks on the curve indicate that the stress will increase further with the progress of deformation. Critical speed defining the transition from plasticity to brittleness is represented by compression speed v, and not the strain rate $\dot{\varepsilon}$. The reason will be illustrated in section V of this paper. In the region of brittleness, where $v > v_c$, p^* decreases with increasing v, while p_* increases, till v reaches a certain value v_c'. If v exceeds v_c', p^* and p_* come to almost the same value which changes only slightly with v. In such a case successive fractures took place, not intermittently, but continuously, and the broken ice grains adhere together, stretching out from the top or the bottom of the snow cylinder towards the outside in a tongue like fashion. This deformation type shall be denoted as brittle deformation of the second type and will be distinguished from the brittle deformation where $v_c < v < v_c'$.

IV. Critical Speed

The critical speed v_c for the transition from plasticity to brittleness decreases with the temperature T, but changes only slightly in the range from 0 to -30°C. It also depends on the nature of snow. Here, experimental snow was only compact snow and the density ρ ranged from 0.15 to 0.45 g/cm^3. v_c inereased with ρ. The dependence of v_c on T and ρ can be roughly expressed by the relation

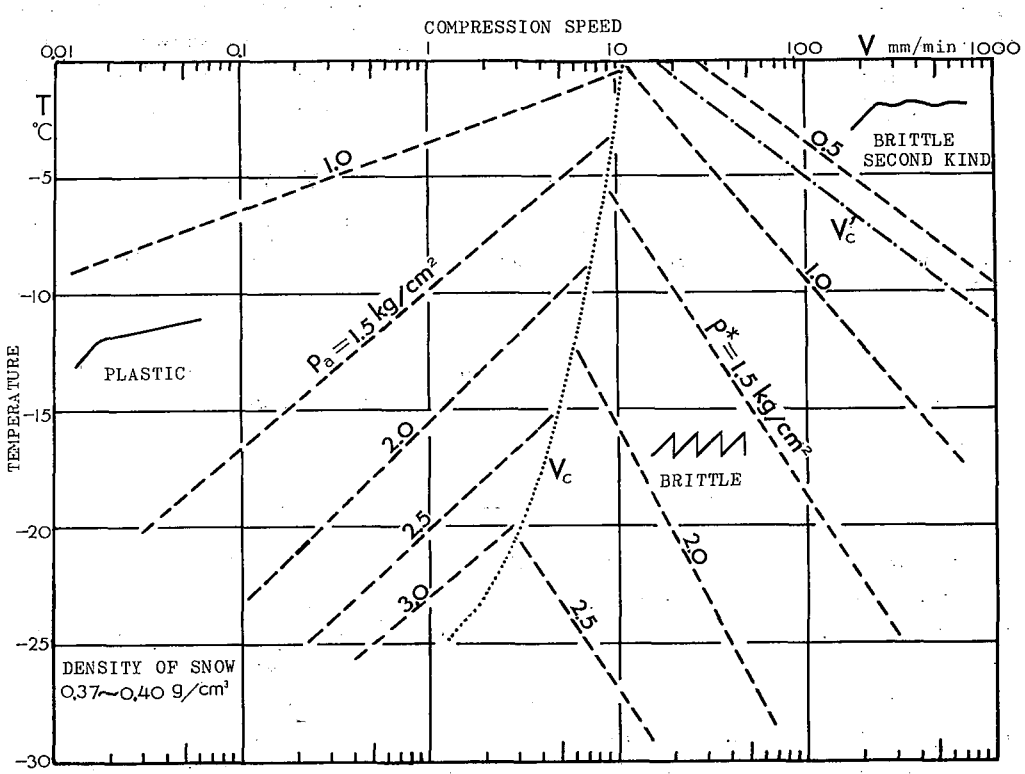

Fig. 4. Relations of p_a, p^* to T and v for the density of 0.37~0.40 g/cm³.
p_a, Compressive stress at 5% strain for plastic deformation;
p^*, Compressive strength for brittle deformation;
v_c and v_c', Critical speed for transition between two deformation types

$$v_c = 0.4\,T + 20\,\rho + 3\,, \qquad (1)$$

where v_c, T and ρ should be respectively counted by the units of mm/min, °C and g/cm³. The dotted curve drawn lengthwise through the diagram of Fig. 4 gives the $v_c - T$ curve for the snow of $\rho = 0.37 \sim 0.4$ g/cm³.

In general plastic deformation takes place uniformly along the entire body. Hence it may be expected that strain rate $\dot{\varepsilon} = \frac{v}{l_0}$ (where l_0 is the original length of snow cylinder) seems more suitable as the critical speed. However, it was found from the following experiments that the critical speed should be represented by the compression

Table 1. The change of the critical speed for transition from plasticity to brittleness on the original length of snow cylinder

T	ρ	Original length	v_c Compression speed	$\dot{\varepsilon}_c$ Strain rate
−4°C	0.28 g/cm³	14 cm	nearly 7 mm/min	nearly 0.5 min⁻¹
−4°C	〃	1	〃 5	〃 5.0
−1°C	0.23	15	〃 7	〃 0.47
−1°C	〃	4	〃 5	〃 1.25

speed. Under the same conditions of temperature and density the value of critical speed was obtained for snow cylinders of various original lengths, as shown in Table 1.

v_c changes only slightly, but $\dot{\varepsilon}_c$ changes largly with the length. Therefore, the compression speed v_c is more suitable for the critical speed than the strain rate $\dot{\varepsilon}_c$.

V. Some Considerations on the Critical Speed

Here it becomes a subject of discussion that the critical speed for snow is a significant quantity and its numerical value is several mm/min. The author suggests that it has a close relation with the internal structure of snow, that is, the network connections of ice grains.

In the case of brittle deformation the compression speed v is related to the time interval t^* from one fracture to the next fracture and the change x^* of length during t^* by

$$v = \frac{x^*}{t^*}. \tag{2}$$

Though the compression speed v is given by external conditions such as experimental procedures, both x^* and t^* are characteristic for the property of snow; x^* is defined by the geometry of the network connections, and t^* by the physical property of the ice.

The above circumstances shall be illustrated in more detail by using a schematic picture as shown in Fig. 5. It gives a microscopic change around the end portion of the compressing snow. A rigid compression plate touches the network of lines which represents the texture of snow. The real network of ice grains composing the snow as shown in the microphotograph of Fig. 3 a are replaced by lines AB, BC, CD, DE, etc. The compression plate is moving towards the snow at a constant speed v. Now, it reaches a front X. The ice grains AB suffer various mechanical actions such as compression, tension, bending or torsion, even though the whole mass is compressed. In consequence the joints B which are the nearest ones to X are fractured and the ice grains AB are taken to pieces. Actually fracture occurs at the end portion of the snow cylinder as seen in Figs. 2 c and d. As the movement of the compression plate progresses, the ice grains AB are ejected or packed in the centre portion. Next, the compression plate reaches a front Y near the plane connecting the previously broken joints B. Then, joints C are fractured in turn. The intermittent fractures take place by the repetition of such processes.

The space interval from X to Y corresponds to x^*. Therefore, x^* is almost the same as the interval between neighbouring joints, that is, the length l of an ice grain. l is distributed in a certain range (Kinosita, 1960). Within the network each interval stands towards any direction with equal probability and the strength for the fracture of each joint is strongly influenced by the type of mechanical action on it such as compression, tension, bending and torsion. Taking these conditions into account, the value of x^* is assumed to be in the order of the length l of an ice grain.

The observed results of the mean length $\bar{l}$ and the mean thickness $\bar{d}$ of ice grains, the compression speed v, the mean value $\bar{x}^*$ of x^* and the mean value $\bar{t}^*$ of t^* for the density

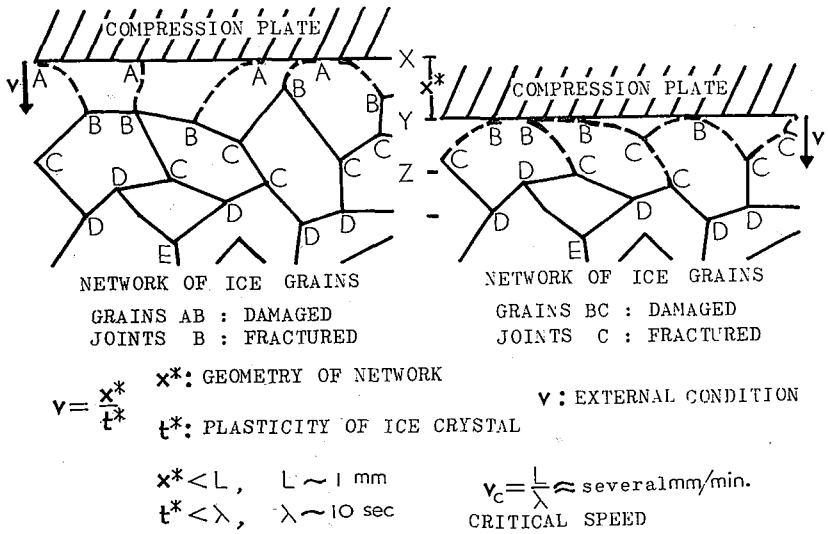

Fig. 5. Schematic pictures representing the compression of network of ice grains

of snow of 0.23, 0.27 and 0.36 g/cm^3 are presented in Table 2. Except for the value of v close to v_c, $\bar{x}^*$ does not change so much as v or t^* and ranges from the same order to a few times of $\bar{l}$. However, when v is equal to v_c, $\bar{x}^*$ becomes larger. The maximum value of x^* is larger than 1 mm which is several times larger than $\bar{l}$. In such a case fractures should take place passing over several joints, where ice grains are more thinly scattered than elsewhere. Wakahama (1960) named those regions weak lines. According to his experiments their intervals are a few milimeters. In the case of the compression at v_c the maximum value of x^* appeared at the final stage of brittle deformation amounted sometimes to few milimeters.

Though the details cannot be completely explained, it seems that the experimental values of x^* might support the above mentioned hypothesis, in which, x^* is closely related to the geometry of the network of ice grains.

After fracture occurs, compressive stress again begins to increase as illustrated in the schematic diagram of Fig. 1 c. This increase depends on the strain rate $\dot{\varepsilon}$ of the whole snow mass. When the ice grains enters the stressed state, dislocations in the basal plane are generated within them. The moving velocity of the dislocation depends on the shear stress acting across the basal plane. When time exceeds a certain limit from one fracture to the next fracture, all of the dislocations pass through the ice grain. As a result plasticity predominates brittleness. As shown in Table 2, t^* increases with the decreasing v. When v equals v_c, t^* amounts to 10 seconds or so. On the other hand, according to Wakahama (1962) the moving velocity of dislocation is 10~60 μ/sec. Since the breadth of each ice grain is in the order of 0.1~0.6 mm for the compact snow of ρ=0.15~0.45 g/cm^3 (Kinosita, 1960), 10 seconds or so is required for the dislocation to pass through the ice grain to the end. These facts are suggestive of the existence of a maximum value on t^* over which plasticity predominates brittleness.

In the curve of resistive force of Fig. 6, where v equals v_c, the time interval t^*

Table 2. Relations of the mean values of x^* and t^* to v for various ρ

ρ	l	d	v	$\bar{x}^*$	Max of x^*	$\bar{t}^*$	Max of $\bar{t}^*$
0.23 g/cm³	0.2 mm	0.09 mm	3.8† mm/min	0.5 mm	1 mm	10 sec	16 sec
			7.9	0.74		5.6	
			11.5	0.35		1.8	
			28	0.29		0.52	
0.27	0.26	0.12	4†	0.67	1.2	10.5	19
			5†	0.8	0.9	12	15
			11.5	0.43		5.3	
			20	0.13		0.3	
			28	0.13		0.3	
0.36	0.6	0.22	8†	1.15	1.4	8	10
			15	0.48		1.8	
			25	0.3		0.7	
			28	0.29		0.64	
			35	0.19		0.32	
			41	0.15		0.22	

ρ, Density of snow; l, Length of ice grain; d, Thickness of ice grain; v, Compression speed; x^*, Advancing distance of compression plate from one fracture till the next fracture; temperature, $-1\sim-9$°C

† Critical speed v_c, at first brittle deformation takes place and after a certain time it turns into plastic deformation. (Fig. 6)

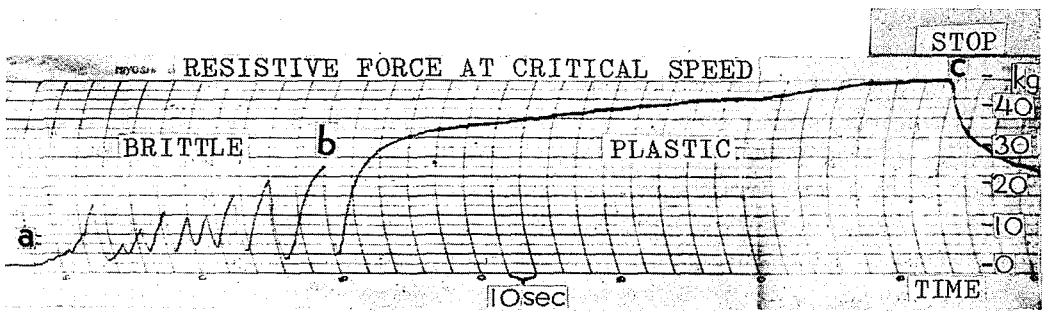

Fig. 6. Curve of the resistive force at the critical compression speed v_c.
a, start; b, final fracture; a~b, brittle deformation; after b, plastic deformation; c, stop; after c, relaxation curve.
Original density of snow: 0.27 g/cm³. Temperature: −2°C.
Compression speed: 4 mm/min

from one fracture to the next fracture becomes larger as compression progresses, and finally fracture discontinues, and turns into plastic deformation. The curve of Fig. 6 gives the data of the uppermost line of Table 2. The maximum value of t^* which appeared at the final stage of brittle deformation amounted to 16 seconds.

If the maximum values of x^* and t^* are denoted respectively by L and λ, the critical speed v_c should be represented by

$$v_c = \frac{L}{\lambda} . \tag{3}$$

Since the value of L and λ are respectively 1 mm or so and 10 sec or so, the numerical value of v_c is equal to several mm/min. This agrees very well with the experimental results.

Generally in bulk material transition phenomena between plasticity and brittleness can be defined by using the strain rate $\dot{\varepsilon}$, and not the displacement speed v, while in the case of snow it is the opposite. This is due to the fact that x^* is related only to the geometry of the network, in other words, the lengths of ice grains and is independent of the strain ε, namely, the ratio for the change in length to the whole length.

VI. General View of Experimental Results

Experimental results obtained to date (Kinosita, 1957, 1958, 1960) will be expressed here by several formulas according to the schematic representations of Figs. 1 c and d. The ranges used for temperature T°C, density ρ g/cm^3 and compression speed v mm/min were respectively $0 \sim -30$, $0.15 \sim 0.45$ and $0.01 \sim 1\,000$.

Compressive stress p_a at 5% strain for plastic deformation

In the case of plastic deformation compressive stress continues to increase as long as compression progresses. Here, an experimental formula will be given for the values p_a at 5% strain. The increase of stress depends on strain rate $\dot{\varepsilon}$, and not the compression speed v. The relation of p_a kg/cm^2 to T°C, ρ g/cm^3 and $\dot{\varepsilon}$ sec^{-1} is given by

$$\log p_a = -0.03\,T + 4.6\,\rho + 0.13 \log \dot{\varepsilon} - 1.6 , \tag{4}$$

where $\dot{\varepsilon}$ is less than about 10^{-3} sec^{-1} for a snow cylinder of 10 cm in length. p_a increases with increasing ρ and $\dot{\varepsilon}$, and decreasing T. In Fig. 4 such a relation for the snow of $\rho = 0.37 \sim 0.4$ g/cm^3 is shown. Here, the group of broken lines within the region of plasticity gives the dependencies of p_a on T and v. The numerals attached to them represent the value of p_a.

Compressive strength for brittle deformation

Compressive strength p^* is distributed over a rather wide range. The relation of p^* kg/cm^2 to T°C, ρ g/cm^3 and v mm/min should be represented roughly by

$$p^* = \rho^3 (27 - T - \log v) , \tag{5}$$

where v lies between v_c and v_c'. p^* increases with increasing ρ and T, and decreasing v. When v exceeds v_c', p^* maintains almost the same value as that of $v = v_c'$. In Fig. 4 such a relation for the snow of $\rho = 0.37 \sim 0.4$ g/cm^3 is shown. There, the group of broken lines within the region of brittleness give the dependencies of p^* on T and v. The numerals attached to them represent the value of p^*.

Visco-elastic quantities

Generally deformation of visco-elastic material exhibits elasticity only at the beginning period, and soon turns to plasticity. Such behavior could be represented by using a simple rheological model, *i.e.* the Maxwell model.

$$\dot{p} = E\dot{\varepsilon} - \frac{E}{\eta} p , \tag{6}$$

where E and η are respectively the elastic constant and viscosity. Within a small strain, $\dot{\varepsilon}$ is regarded as constant here, hence

$$p = E\tau\dot{\varepsilon}\left\{1-\exp\left(-t/\tau\right)\right\}, \tag{7}$$

where $\tau(=E/\eta)$ is the relaxation time. Therefore, for the beginning stage,

$$p \sim E\tau\dot{\varepsilon}t, \tag{8}$$

and for the final stage, $$p \sim E\tau\dot{\varepsilon} \quad \text{or} \quad \eta\dot{\varepsilon}. \tag{9}$$

When compression is discontinued ($\dot{\varepsilon}=0$), the stress decreases as follows.

$$p = p_0 \exp\left(-t/\tau\right), \tag{10}$$

where p_0 is the value of stress at the stoppage.

The values of E, η and τ were computed from the curves of resistive force following the above eqs. (8), (9) and (10) respectively.

E (*elastic constant*). E ranged from 10^6 to 10^9 dyne/cm^2, and increased with the increasing density of snow ρ and strain rate $\dot{\varepsilon}$, but almost independently of the temperature T used. The relationship can be represented by

$$\log E = 5.9\,\rho + 0.24 \log \dot{\varepsilon} + 6.4, \tag{11}$$

where E, ρ and $\dot{\varepsilon}$ are respectively counted by the units of dyne/cm^2, g/cm^3 and sec^{-1}.

η (*viscosity*). This was computed only for plastic deformation. Stress at 5% strain, p_a, should be taken here as the final stress of eq. (9), though the stress increased further with the progress of compression. η ranged from 10^8 to 10^{11} dyne·sec/cm^2, and increased with decreasing T and $\dot{\varepsilon}$, and increasing ρ. The relationship can be represented by

$$\log \eta = -0.03\,T + 4.6\,\rho - 0.87 \log \dot{\varepsilon} - 1.6, \tag{12}$$

where η, T, ρ and $\dot{\varepsilon}$ are respectively counted by the units of dyne·sec/cm^2, °C, g/cm^3 and sec^{-1}.

τ (*relaxation time*). Actually the stress relaxation did not yield eq. (10). Some researchers (Ôura, 1957; Shinojima, 1966; Kinosita, 1957) suggested the formula

$$p = p_0 \exp\left(-\sqrt{t/\tau}\right) \tag{13}$$

Also, the author (Kinosita, 1965) suggested the formula

$$p = p_0 \left(ct+1\right)^{-\frac{1}{2}}, \tag{14}$$

where c was constant ($0.05 \sim 0.5\,\text{sec}^{-1}$). The rate of stress decrease depended strongly upon the strained amount besides ρ, T and $\dot{\varepsilon}$ (Kinosita, 1960). If the strained amount was within 10%, τ ranged from 10 seconds to several minutes.

The representation of the increase of stress with time by using a visco-elastic formula

Generally it is expressed by

$$p(t) = E\varepsilon(t) - \int_0^t \mathrm{f}(t-t')\,E\varepsilon(t')\,\mathrm{d}t', \tag{15}$$

where f is the so called memory function. Using the stress relaxation formula (14),

$$\mathrm{f}(x) = -\frac{1}{2}\,c\left(cx+1\right)^{-\frac{3}{2}} \tag{16}$$

At constant speed compression ($\varepsilon = a\ t$, where a is a constant), eq. (15) turns to

$$p(t) = Ea\frac{2}{c}\left\{1-(ct+1)^{-\frac{1}{2}}\right\}. \tag{17}$$

This formula agrees well with the actual increase of compressive stress.

VII. Special Experiments

Transformation of snow into ice by a large plastic compression

On slow speed compression plastic deformation takes place as long as compression progresses. At the final stage snow is transformed into ice. As a natural phenomena such transformation makes its appearance in glaciers or ice caps, where the ice crystals at the depths have suffered innumerable years of plastic deformation under the load of the upper layer.

In the cold room the transformation of snow into ice was produced by using an air-hydraulic type compression apparatus of a large loading capacity (Kinosita, 1962). The original snow cylinder of 10~15 cm in length was made finally into a very thin ice sheet of 0.08~2 cm thick. The internal texture changes of snow during the compression were studied by microscopic observations of thin sections which were taken from the uppermost portion of the sample at several stages in succession.

At the first stage, when the increasing density ρ' with compression reached about 0.6 g/cm^3, internal changes such as given in schematic picture of Fig. 1 b (upper) proceeded; these changes were studied in detail by Wakahama (1960).

At the second stage, when ρ' reached about 0.8 g/cm^3, the ice grains came into contact with each other more frequently and increased in size by sintering (Fig. 7 a), where the marks **f** show the portions of contact. The air space became more narrow and finally came to be divided into isolated air bubbles (Fig. 7 b), where the mark **x** shows the air bubbles standing along the grain boundaries, and the mark **y** shows the air bubbles included within the crystal. At such a stage the compressed sample could not be referred to as snow but should be referred to as ice.

At the final stage, when ρ' was close to the density of ice, these air bubbles divided into smaller ones, and scattered within the mass of ice in a cloud like fashion. The grains began to break up into smaller units (Fig. 7 c). This crystal division was probably due to the appearance of new crystals by recrystallization.

In Fig. 8 the compressive stress p is plotted against ρ', the density of snow increasing with the compression. The left end of each curve shows the original density. As long as ρ' does not exceed 0.85 g/cm^3, the relationship between p kg/cm and ρ' g/cm^3 can be given by

$$\log p = -1.1+3.7\,\rho' . \tag{18}$$

In a glacier or ice cap in the polar region the density of snow at 50 m deep below the surface is 0.79 g/cm^3 and the layer suffers a pressure of 3.5 kg/cm^2 according to the theory of densification (Shumsky, 1960), while eq. (18) gives the pressure at $\rho' = 0.79$ g/cm^3 where the sample suffers the pressure of 65 kg/cm^2. This is about 20 fold in largeness. The difference is due to the compression speed: Stress increases with the speed as seen in eq. (4).

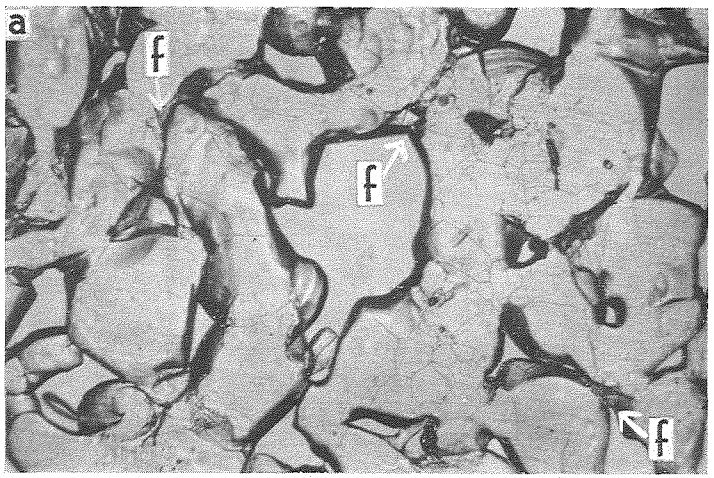

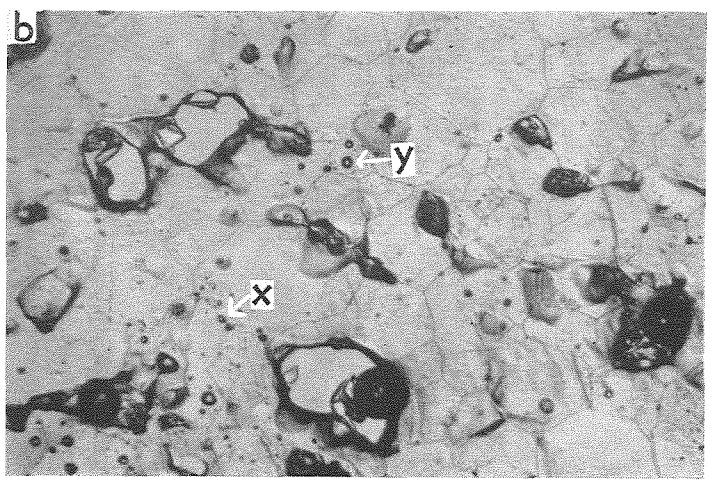

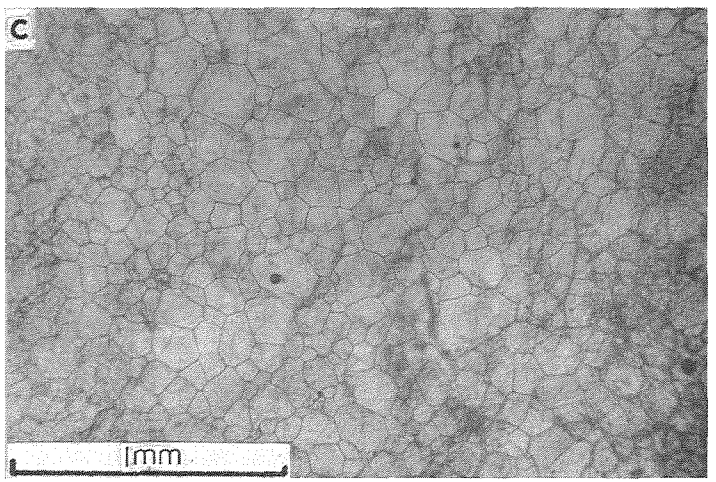

Fig. 7. Thin sections of snow which were undergoing transformation into ice under large plastic compression, original density : 0.35 g/cm^3.

a : Increasing density $\rho = 0.64$ g/cm^3, strain $\varepsilon = 0.67$. f, contact of ice grains,

b : $\rho' = 0.78$, $\varepsilon = 0.87$, x, air bubbles standing along the grain boundary ; y, air bubbles included within the ice crystal,

c : $\rho' \approx$ density of ice, $\varepsilon = 0.99$

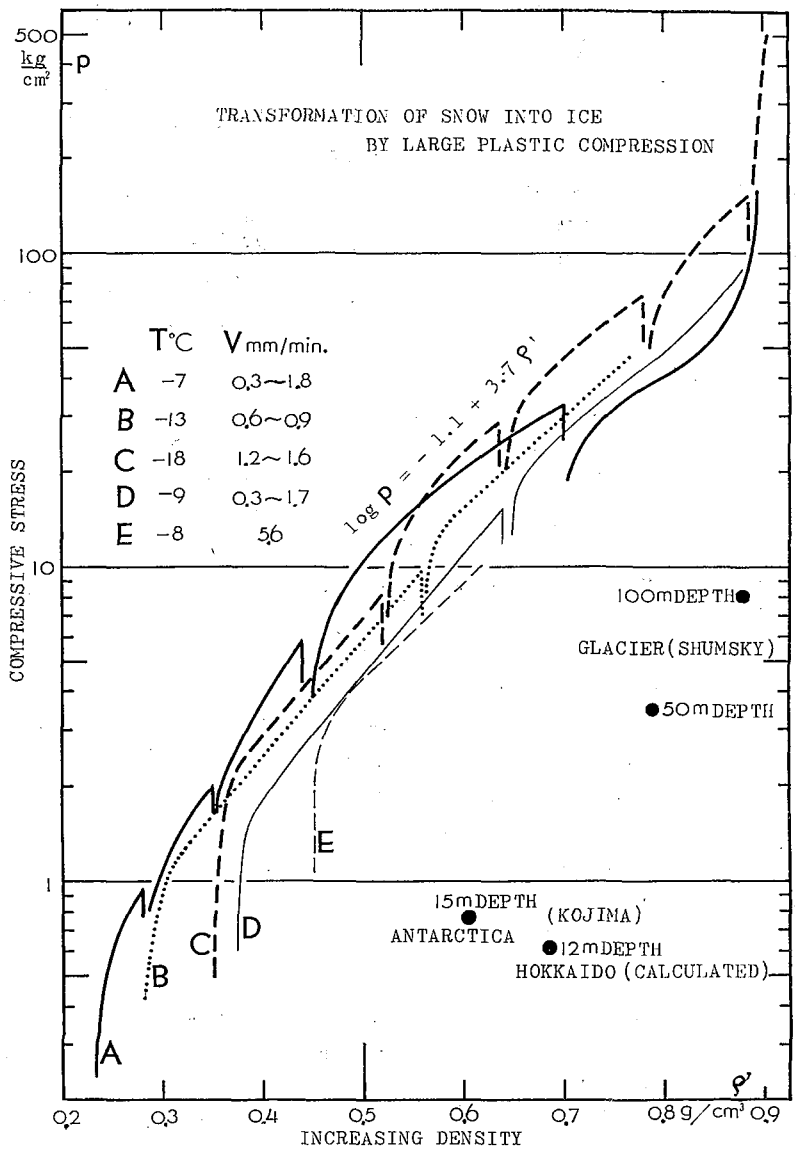

Fig. 8. Relation of compressive stress p to increasing density ρ' in transformation of snow into ice by a large plastic compression

In the experiment the strain rate $\dot{\varepsilon}$ was approximately 10^{-4} sec^{-1}, while in the glacier or the ice cap it is 10^{-9} sec^{-1} or thereabouts.

The numerical values obtained from the densification theories of Shumsky (1960) and Kojima (1964) are plotted in the graph of Fig. 8.

Observation of the top surface of a snow cylinder compressed by a transparent plate

On brittle deformation of a snow cylinder the broken ice grains seemed to be ejected outwardly, judging from the side view, but they were packed together also at the centre of the top surface. This fact was found by observations of the top surface

from above, compressing the snow cylinder by a transparent plate (Kinosita, 1964).

As the compression progresses, the region of the packed ice grains enlarges to form finally a cone, the generating line of which, lies in the direction of maximum shear stress. Until the formation of the cone, the snow continues to break down on the lower and the side surface of the region. After the formation of such a cone several vertical splits, appear through the snow cylinder. This region at the beginning stage is presented in the schematic figure of Fig. 1 a (below) as a dotted portion of the uppermost of the compressed snow cylinder.

This is suggestive of the existence of shear stress in a radial direction across the end surface.

Intrusion of a rigid cone into snow

By forcing rigid cones of various apex angles into snow an investigation was conducted on how the broken ice grains were related to the shear stress across the upper end surface (Kinosita, 1965). The region made by packing the broken ice grains developed in two different ways: One was made besides the cone (for apex angle θ of smaller than 90°, Fig. 2 g), and the other under the cone (for θ of larger than 90°, Fig. 2 f). From these observations it may be considered that when the shear stress is smaller than normal stress across the cone surface, the broken ice grains are packed under the cone while in the opposite case they are carried backwards.

With plastic deformation, snow layers lengthened and bent (Fig. 2 e): Most of the ice grains in the snow near the cone underwent a basal slip. From these experiments the following relations were obtained between the force F kg, the vertical angle of the cone θ°, the snow density ρ g/cm^3 and the subsiding distance of the apex of cone under the snow surface z cm.

For brittle deformation $$F = 7\theta^{\frac{5}{3}}\rho^3 z^2, \tag{19}$$

For plastic deformation $$F = 14\theta^{\frac{5}{3}}\rho^3 z^2. \tag{20}$$

Compression of wet snow

When snow becomes wet, it becomes very easy to compress (Kinosita, 1963; Wakahama, 1965). On brittle deformation in the region of $v_c < v < v_c'$ intermittent fractures take place and become restricted within more narrow limits with the increase of the free water content in the wet snow. The other mechanical behaviors change to a considerable extent. Also, the rate of the metamorphism of the internal texture becomes extremely rapid (Wakahama, 1965). In addition, many interesting phenomena have already been found for wet snow (Huzioka, Tabata and Kinosita, 1963), but a detailed study on the compression has not yet been conducted.

VIII. Conclusion

The mechanical behavior of snow shows a characteristic visco-elasticity. It was found that such properties were due to the internal structure of snow, namely the network connections of ice grains. The brittleness given at high speed compression depends on the geometry of the network. The plasticity given at slow speed compression depends on the rate of the stress relaxation within the ice grains.

Acknowledgments

The author wishes to express his hearty thanks to Prof. Z. Yosida, Prof. D. Kuroiwa and Dr. G. Wakahama for their valuable comments.

References

1) HUZIOKA, T., TABATA, T. and KINOSITA, S. 1963 "Snow jam" in lake Oze. *Low Temp. Sci.*, **A 21**, 95–115.*
2) KINOSITA, S. 1957 The relation between the deformation velocity of snow and two types of its deformation (plastic and destructive). *Low Temp. Sci.*, **A 16**, 139–166.*
3) KINOSITA, S. 1958 The relation between the deformation velocity of snow and types of its deformation. II. *Low Temp. Sci.*, **A 17**, 11–30.*
4) KINOSITA, S. 1960 Natural changes in the microscopic texture of snow (observation by the use of thin sections). *Low Temp. Sci.*, **A 19**, 111–118.*
5) KINOSITA, S. 1960 The hardness of snow. *Low Temp. Sci.*, **A 19**, 119–134.*
6) KINOSITA, S. 1960 The relation between the deformation velocity of snow and the types of its deformation. III. *Low Temp. Sci.*, **A 19**, 135–146.*
7) KINOSITA, S. 1962 Transformation of snow into ice by plastic compression. *Low Temp. Sci.*, **A 20**, 131–157.*
8) KINOSITA, S. 1963 Compression of snow immersed in water of 0°C. *Low Temp. Sci.*, **A 21**, 13–22.*
9) KINOSITA, S. 1964 Observation of the end surface of a snow cylinder compressed by a transparent plate. *Low Temp. Sci.*, **A 22**, 73–82.*
10) KINOSITA, S. 1965 Intrusion of a rigid cone into snow. *Low Temp. Sci.*, **A 23**, 17–37.*
11) KINOSITA, S. and WAKAHAMA, G. 1960 Thin sections of deposited snow made by the use of aniline. *Contr. Inst. Low Temp. Sci.*, **15**, 35–45.
12) KOJIMA, K. 1964 Densification of snow in Antarctica. *Antarctic Res. Ser.*, **2**, 157–218.
13) ÔURA, H. 1957 On the force with which a beam supports the ceiling of a snow cave. *Low Temp. Sci.*, **A 16**, 55–72.*
14) SHINOJIMA, K. 1966 Study on the visco-elastic deformation of deposited snow. *In* Physics of Snow and Ice, Part 2 (H. ÔURA, *ed.*), Inst. Low Temp. Sci., Sapporo, 875–907.
15) SHUMSKY, P. A. 1960 Density of glacier ice. *J. Glaciol.*, **3**, 568–573.
16) WAKAHAMA, G. 1960 Internal strain and changes in the microscopic texture of snow caused by compression. I. *Low Temp Sci.*, **A 19**, 37–72.*
17) WAKAHAMA, G. 1962 On the plastic deformation of ice. III. *Low Temp. Sci.*, **A 20**, 101–116.*
18) WAKAHAMA, G. 1965 Metamorphism of wet snow. *Low Temp. Sci.*, **A 23**, 51–66.*
19) WAKAHAMA, G. 1966 Compression of thin section of snow. *In* Physics of Snow and Ice, Part 2 (H. ÔURA, *ed.*), Inst. Low Temp. Sci., Sapporo, 909.

* In Japanese with English summary.